REGULAR PAPER
DOI: 10.1007/s12541-018-0110-3
ISSN 2234-7593 (Print) / 2005-4602 (Online)

An Investigation of Surface Roughness in Ultrasonic Assisted Dry Grinding of 12Cr2Ni4A with Large Diameter Grinding Wheel

Hai-Feng Chen[1,2], Jin-Yuan Tang[2,#], Wen Shao[2,#], and Bo Zhao[3]

1 Hunan Provincial Key Laboratory of High Efficiency and Precision Machining of Difficult-to-cut Materials, Hunan University of Science and Technology, Xiangtan, Hunan, 411201, China
2 State Key Laboratory of High Performance Complex Manufacturing, Central South University, Changsha, Hunan, 410083, China
3 School of Mechanical and Power Engineering, Henan Polytechnic University, Jiaozuo, Henan, 454000, China
Corresponding Author / E-mail: jytangcsu_312@163.com, ORCID: 0000-0001-7186-1316
E-mail: shaowen_2013@163.com, ORCID: 0000-0002-5654-546X

KEYWORDS: Ultrasonic assisted dry grinding, Steel, Large grinding wheel, Surface roughness

Ultrasonic assisted dry grinding (UADG) is a novel green manufacturing technology for decreasing the negative environment impact of cutting fluids and improving the surface characteristics. In this study, the influences of the ultrasonic amplitude, grinding depth and grinding velocity on the surface roughness in ultrasonic assisted dry grinding of 12Cr2Ni4A with a large CBN grinding wheel were investigated. Due to the Poisson effect, the ultrasonic assisted dry grinding using a large diameter grinding wheel is the combination of axial ultrasonic assisted grinding and radial ultrasonic assisted grinding. The results indicated that the main axial ultrasonic component tended to smooth the surface topography by increasing the interaction overlap of the adjacent cutting traces, but it would result in more side flow/ploughing on the surface at a larger ultrasonic amplitude; the radial ultrasonic component exerted a function on the increase of the surface roughness through deepening the individual grinding trajectories. Thus, the surface roughness decreased first and then increased with the increase of grinding depth due to the combined contribution of axial and radial vibrations. However, the improving effect of ultrasonic vibration on the surface roughness gradually weakened with the increase of grinding velocity. Under proper operating parameters, surface roughness obtained in ultrasonic assisted dry grinding can be reduced up to 30% compared with that of common dry grinding.

Manuscript received: November 23, 2017 / Revised: January 11, 2018 / Accepted: February 9, 2018

1. Introduction

The cutting fluids have been extensively used in the metal grinding process due to its good performance in cooling, cleaning, lubricating and antirusting. However, high costs and associated environmental problems have been associated with the use of a large quantity of coolant-lubricants.[1] Dry grinding (DG) technology is a fundamental solution to eliminate the environmental and economic problems caused by cutting fluids. Nevertheless, without sufficient cooling and lubrication, the instant high temperature and considerable heat generated in grinding process would lead to severe burns of the machined surface. Over the years, ultrasonic assisted machining technologies such as ultrasonic drilling,[2,3] ultrasonic vibrating abrasive slurry jet machining,[4,5] and ultrasonic welding[6] have been emerged to improve the surface integrity and decrease the negative environment impact of cutting fluids. Previous research indicated that ultrasonic vibration grinding methods could greatly lower the temperature in the grinding zone.[7] The UADG technique works by superimposing high frequency (16-40 kHz) and low amplitude (2-30 μm) in the feed or cross feed direction to the tool[8-10] or the workpiece.[11,12] It was well documented that UADG could reduce thrust force and heat generation as well as improve surface quality under proper operating parameters compared with that of conventional dry grinding. Tawakoli and Azarhoushang[7] demonstrated that the thermal damage of the workpiece could be eliminated and the normal and tangential grinding forces reduced by 60-70% and 30-50% respectively with the aid of ultrasonic vibration. Paknejad et al.[13] measured the temperature history and distribution of workpiece during ultrasonic assisted dry creep feed up grinding and indicated that the ultrasonic vibration resulted in a dramatic decrease in maximum temperature by 25.91% compared with DG. Experimental results of Chen et al.[14] on ultrasonic assisted dry grinding of carbon steel showed a maximum reduction of 20% in surface roughness could be achieved compared with that of DG and the values of the parameters R_k, R_{pk} and R_{vk} of the Abbott-Firestone curve in UADG were smaller than those in DG.[15] Wang et al.[16] also reported that ultrasonic vibration frequency and amplitude had a significant influence on the material removal, grinding force, surface morphology and roughness. It was found that higher amplitude and frequency tended to produce a better surface.

Meanwhile, the resonance of sonic wave vibration is the key technology in the ultrasonic assisted grinding. If the ultrasonic is superimposed to the workpiece, then each ultrasonic vibration system must be individually designed to match the natural frequencies of the workpiece as the ultrasonic vibration system is determined by the material and structure of the workpiece. This makes it difficult and expensive to design an ultrasonic vibration system. Instead, if the ultrasonic is superimposed on the grinding wheel, these disadvantages can be eliminated. However, as ultrasonic assisted grinding usually operates with the diameter of the grinding wheel in the vicinity of 10 mm, it is mainly applied in the processing of micro components.[17] The diameter of the grinding wheel used to machine conventional engineering parts is normally greater than 100 mm in order to improve the machining efficiency. Although the ultrasonic vibration is designed in one-wave length resonance, it should be noted that pure-longitudinal waves can only exist in solids where the dimensions are very large compared with the longitudinal wavelength. If not, due to the Poisson effect, another ultrasonic vibration is simultaneously generated in the radial direction at the same frequency but with a much smaller amplitude.[18,19] The amplitude in the radial direction is proportional to the diameter of the grinding wheel.[20] Therefore, the ultrasonic assisted grinding using a large diameter grinding wheel is just the combination of axial ultrasonic assisted grinding and radial ultrasonic assisted grinding. Since the amplitude in the radial direction is much smaller than that in the axial direction, it is different from two-dimensional ultrasonic assisted grinding[21] or elliptical ultrasonic assisted grinding[22] where the amplitudes in different directions are usually identical.

As indicated by the literature review above, many researches have been done on the UADG, but the effect of ultrasonic assisted dry grinding with a large diameter grinding wheel on surface roughness has not been studied yet. In this paper, an experimental platform was set up firstly to perform ultrasonic assisted dry grinding with a large diameter grinding wheel. Then, the influences of the vibration amplitude, the depth of grinding and the grinding velocity on the surface roughness were systematically studied. Finally, the formation mechanism of the surface roughness was discussed from the view point of the effect of ultrasonic in different directions on the grain movement track.

2. Kinematic Characteristics

Fig. 1 shows the schematic view of the UADG. A resin-bonded CBN grinding wheel with a large diameter vibrating ultrasonically along its own axial with frequency and amplitude of f and A_Z rotates clockwise with rotation speed of V_s. As shown in Fig. 1, V_w is the feed speed of

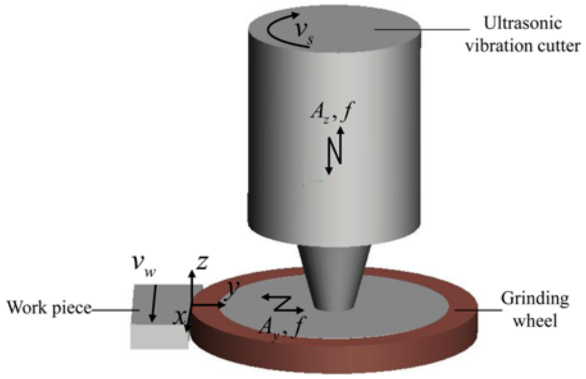

Fig. 1 Schematic diagram of UAG

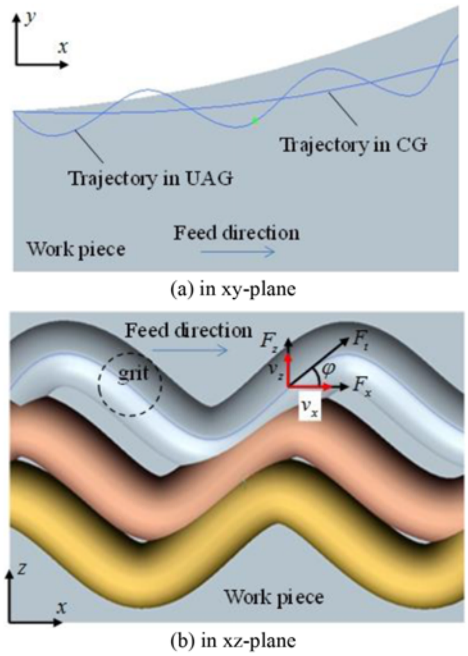

Fig. 2 Kinematics of cutting action in ultrasonic assisted grinding

workpiece, and a_p is the grinding depth. As mentioned previously, due to the Poisson effect, another ultrasonic vibration is simultaneously generated in the radial direction at the same frequency of f but with a much smaller amplitude of A_y. In the current work, to verify this statement, the vibration amplitudes of the grinding wheel in the radial and axial direction were measured using a laser displacement sensor (LK-G10 by KEYENCE), and the test results confirmed that the ultrasonic amplitude was about 3 μm in the radial direction and about 10 μm in the axial direction. Due to the ultrasonic vibration in y-direction, the grinding wheel moves leftward and rightward alternatively in the grinding process. As a result, the grinding depth of UADG changes periodically, resulting in a relative greater maximum depth compared with that of CDG, as shown in Fig. 2(a). The sinusoidal cutting trace of the grinding wheel is generated due to the ultrasonic vibration in z-direction, as shown in Fig. 2(b).

The global coordinate system $Oxyz$ is set with its origin O fixed on the workpiece and coinciding with the grain at the lowest point. The trajectory of grain G can be expressed as

Table 1 Mechanical properties of workpiece (12Cr2Ni4A)

Elastic modulus (GPa)	Density (kg/m^3)	Poisson's ratio	HRC
207	7.84×10^3	0.298	13

Table 2 Machining variables

Experiment	Spindle speed (rpm)	Ultrasonic vibration amplitude (um)	Grinding depth (um)
Group 1	1200	0	5,10,15,20,25,30
Group 2	1200	4	5,10,15,20,25,30
Group 3	1200	7	5,10,15,20,25,30
Group 4	1200	10	5,10,15,20,25,30

Table 3 Machining variables

Experiment	Grinding depth (um)	Ultrasonic amplitude (um)	Spindle speed (rpm)
Group 5	10	0	400,800,1200,1600, 2000,2400
Group 6	10	4	400,800,1200,1600, 2000,2400
Group 7	10	7	400,800,1200,1600, 2000,2400
Group 8	10	10	400,800,1200,1600, 2000,2400

$$\begin{cases} x = v_w t + \frac{d_s}{2}\sin(2\pi v_s t) \\ y = \frac{d_s}{2}(1-\cos(2\pi v_s t)) + A_y\cos(2\pi ft+\phi_0) \\ z = A_z\sin(2\pi ft+\phi_0) \end{cases} \quad (1)$$

The velocities of the tool in the *x*-, *y*- and *z*- directions at time *t*, represented as v_x, v_y and v_z, respectively, can hence be determined by differentiating Eq. (1) with respect to time *t*.

$$\begin{cases} v_x = v_w + \pi d_s v_s\cos(2\pi v_s t) \\ v_y = \pi d_s v_s\sin(2\pi v_s t) - 2\pi fA_y\sin(2\pi ft+\phi_0) \\ v_z = 2\pi fA_z\cos(2\pi ft+\phi_0) \end{cases} \quad (2)$$

The contact length for a single grain can be represented as

$$\begin{aligned} l_k &= \int\sqrt{v_x^2+v_y^2+v_z^2}\,dt \\ &= \int\sqrt{\begin{aligned}&(v_w+\pi d_s v_s\cos(2\pi v_s t))^2+(\pi d_s v_s\sin(2\pi v_s t) \\ &-2\pi fA_y\sin(2\pi ft+\phi_0))^2+(2\pi fA_z\cos(2\pi ft+\phi_0))^2\end{aligned}} \end{aligned} \quad (3)$$

The DG process can be treated as a special case of UADG where $A_y = 0$ and $A_z = 0$. Thus, it is deduced from Eq. (3) that the length of the grain trajectory in UADG is greater than that in DG under the same conditions. However, due to the ultrasonic vibration amplitude on the order of micrometers, the second and third term on the right hand side of Eq. (3) may be overestimated if the grinding velocity is large enough.

3. Experimental Setup and Conditions

The grinding tests were carried out on a 3-axis NC milling machine with the conventional main spindle replaced with an ultrasonic spindle, as shown in Fig. 3. The frequency of ultrasonic spindle is near 25 kHz and the maximum amplitude A_z is around 10 μm. The output ultrasonic amplitude can be adjustable by varying the ultrasonic power. At the lower end of the spindle, a resin-bonded 120# CBN grinding wheel with a diameter of 100 mm was fixed. The workpiece is a plate-shaped

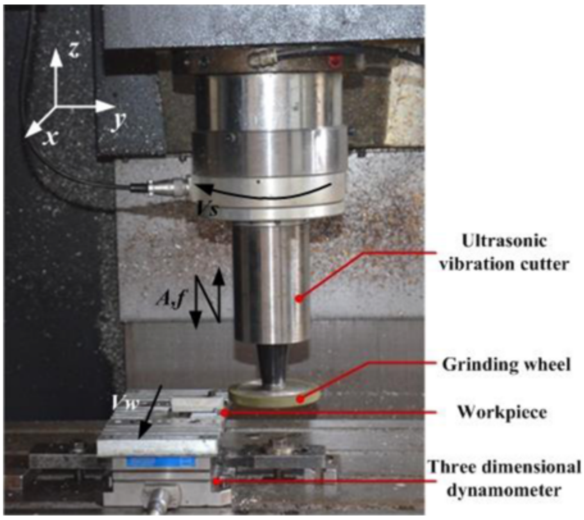

Fig. 3 Experimental set-up for ultrasonic assisted dry grinding

specimen of 12Cr2Ni4A steel (tempering at 140°C) with dimensions of L16 × W9 × T9 mm. The main material properties of it are listed in Table 1.

As shown in Tables 2 and 3, several groups of grinding tests were performed using various grinding depths of 5, 10, 15, 20, 25, and 30 mm, different ultrasonic amplitudes and wheel speeds of 0, 4, 7, 10 um and 400, 800, 1200, 1600, 2000, 2400 rpm respectively. Common grinding tests were performed by switching off the ultrasonic generator. Wheel dressing was carried out prior to each group using a silicon carbide roller with a 100 mm/min feed speed, 2000 rpm spindle speed and 30 μm dressing depth with spark-out.

After the grinding tests, the sample was ultrasonically cleaned for 15 minutes in anhydrous alcohol. A scanning electron microscope (SEM) with various magnifications (2000×) was used to investigate the surface integrity and fracture mode. A white-light interferometer (NT 9100 by Wyko, Co., Ltd.) was employed to measure the three-dimensional surface roughness parameters. To ensure the reliability of the test data, three tests were carried out where each set of process parameters were used to get the average values.

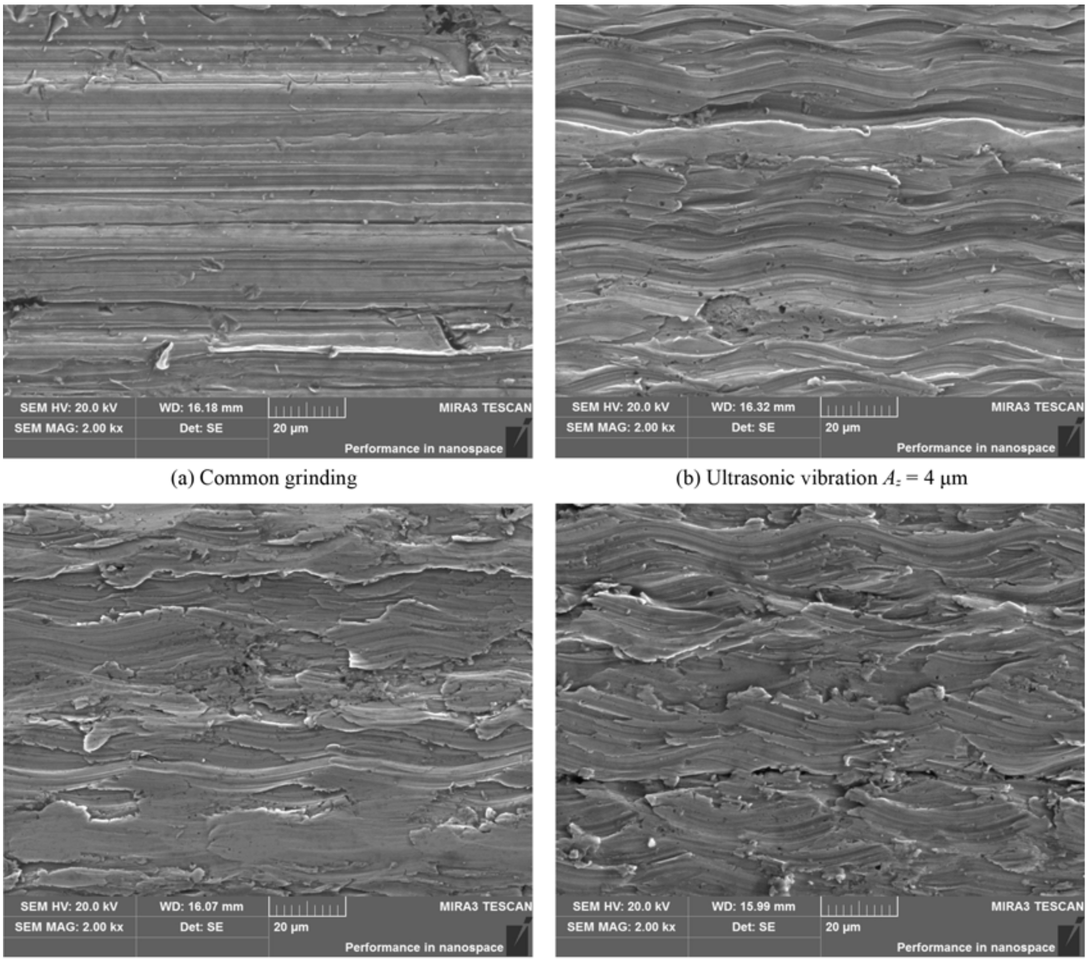

(a) Common grinding (b) Ultrasonic vibration $A_z = 4$ μm

(c) Ultrasonic vibration $A_z = 7$ μm (d) Ultrasonic vibration $A_z = 10$ μm

Fig. 4 SEM images of work surface

4. Results and Discussions

The influences of the ultrasonic vibration on the machining mechanism were investigated. Figs. 4(a) to (d) show the SEM images of typical workpiece surfaces ground by DG and UADG at spindle speed of 1200 rpm and grinding depth of 15 μm. It can be seen that the surfaces ground after UADG have greater levels of overlapping and side flow/ploughing, and the overlapping and side flow/ploughing were aggravated with the increase of vibration amplitude.

The primary reason for this phenomenon is that the tangential grinding direction changes in a sinusoidal pattern as shown in Fig. 2(b). Then, the tangential force F_t can be divided into two parts along the x and z direction, which are respectively given by:[23]

$$\begin{cases} F_x = F_t \cos\varphi \\ F_z = F_t \sin\varphi \end{cases} \tag{4}$$

where φ is the engagement angle which can be obtained by the relative velocity of the abrasive grain in Eq. (2)

$$\varphi = \arctan\left(\frac{v_z}{v_x}\right) = \arctan\left(\frac{2\pi f A_z \cos(2\pi ft + \phi_0)}{v_w + \pi d_s v_s \cos(2\pi v_s t)}\right) \tag{5}$$

Substitute Eq. (5) into Eq. (6), and the following result is obtained.

$$\begin{cases} F_x = F_t \cos\varphi \\ F_z = F_t \sin\left(\arctan\left(\frac{2\pi f A_z \cos(2\pi ft + \phi_0)}{v_w + \pi d_s v_s \cos(2\pi v_s t)}\right)\right) \end{cases} \tag{6}$$

Eq. (6) implies that the ultrasonic vibration amplitude in the axial direction adds additional force in the z-direction. Hence the stress between the grain and the workpiece in the z-direction is increased. Nevertheless, the stress produced by F_z has not reached the fracture stress as the engagement angle is small. Thus, the workpice material flow upheaved and stacked at two sides of the furrows. In addition, the F_z is proportional to the tangential force F_t and amplitude A_z. It is also well known that the cutting forces increase as the grinding depth increases.[24] Therefore, more material piles up to the sides of the groove as the ultrasonic vibration amplitude and the grinding depth increase, resulting in a worse ground surface.

The influences of the vibration amplitude on surface roughness were investigated as well. Fig. 5 shows the surface roughness vs grinding depth at different vibration amplitudes. Experiments were conducted at a spindle speed of 1200 r/min and a feed speed of 300 mm/min. It is evident that the variation trends of the surface roughness in UADG and DG are different. The surface roughness in DG rises against the grinding depth. However, in UADG, the surface roughness first decreases and

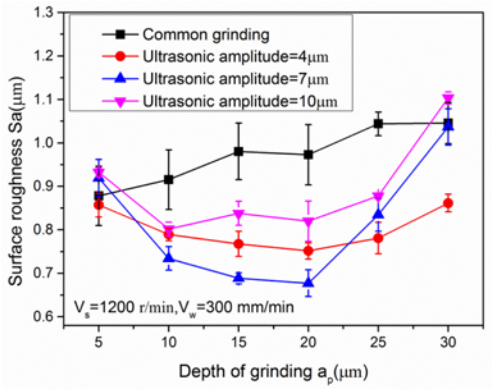

Fig. 5 Surface roughness versus depth of grinding for different ultrasonic amplitudes

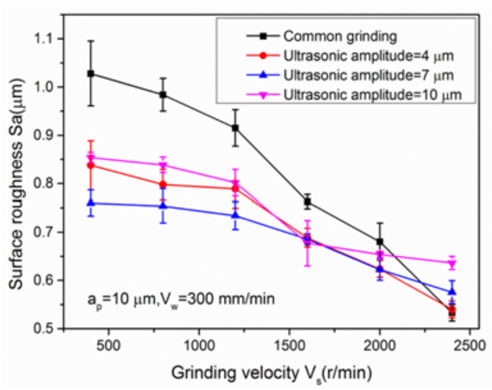

Fig. 6 Surface roughness versus grinding velocity for different ultrasonic amplitudes

then increases with respect to the grinding depth. At the same grinding depth, the situation is more complex depending on the ultrasonic vibration amplitude. For the grinding depth of 5 μm, the surface finish in ultrasonic assisted grinding is improved by 2.4% over the DG at the vibration amplitude of 4 μm. In contrast, the surface finish with ultrasonic assisted grinding technique is worse than that in DG at the vibration amplitude of 7 μm and 10 μm. For the grinding depth in the range of 10-20 μm, the surface roughness with the vibration amplitude of 7 μm is the smallest where a reduction of up to 30% is achieved at the grinding depth of 20 μm. Compared with the vibration amplitude of 4 μm, the effectiveness of UADG is the worst at the vibration amplitude of 10 μm. Once the grinding depth is beyond 20 μm, the surface roughness in UADG increases rapidly. It is worth noting that for the grinding depth of 30 μm, the surface finish with ultrasonic assisted grinding technique is worse than that in DG at the vibration amplitude of 7 μm and 10 μm.

The influences of the vibration amplitude and grinding velocity on the surface roughness were obtained as shown in Fig. 6. The grinding depth of and feed speed were set as 10 μm and 300 mm/min respectively. Obviously, the surface roughness in all the cases presents a similar reduction variation tendency as the grinding velocity increases. The results show that UADG has certain effect in reducing the surface roughness at low grinding velocities. There is a reduction of up to 26%

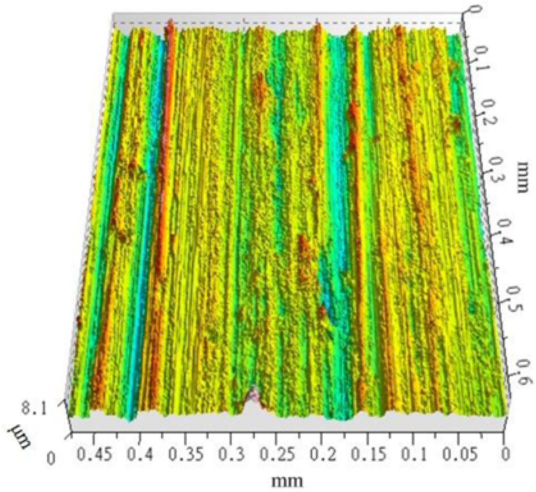

(a) Common grinding (grinding velocity = 1200 rpm, grinding depth = 5 um and feed = 300 mm/min)

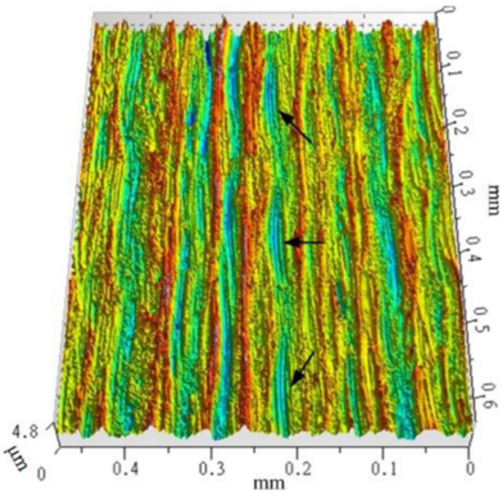

(b) Ultrasonic assisted grinding (grinding velocity = 1200 rpm, grinding depth = 5 um, feed = 300 mm/min, frequency = 25, kHz and amplitude = 4 um)

Fig. 7 Photographs of the ground surface

in surface roughness at thegrinding speed of 400 rpm and vibration amplitude of 7 μm. However, as the grinding velocity increases, UADG's effect gradually weakens, and becomes even worse for the grinding speed of 2400 rpm. At the same grinding velocity, the surface roughness decreases at the beginning and then increases with the increase of ultrasonic vibration amplitude. However, when the grinding velocity exceeds 1600 rpm, the surface roughness increase gradually with the increase of ultrasonic amplitude.

For the results shown in Figs. 5 and 6, the contribution of the UADG with a large diameter grinding wheel to the surface roughness can be accordingly attributed to the overlapping and ploughing conditions in the axial direction, the intermittent cutting conditions in the radial direction. Due to the oscillation in the radial direction, as shown in Fig. 2(a), the tool moves leftward and rightward alternatively in the cutting process, leading to the periodical variation of the depth of grinding in UADG and its maximum value to be greater than that in CG. It can be observed from Fig. 7 that the ground surface after DG consisting of

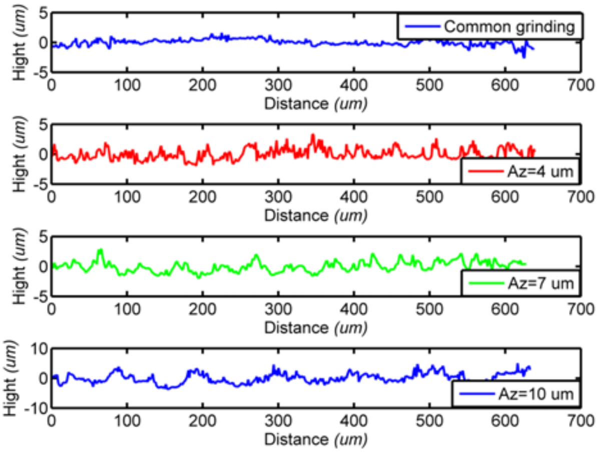

Fig. 8 Surface profiles of the ground workpiece in CDG and UADG (grinding velocity = 1200 rpm, grinding depth = 15 um and feed speed = 300 mm/min)

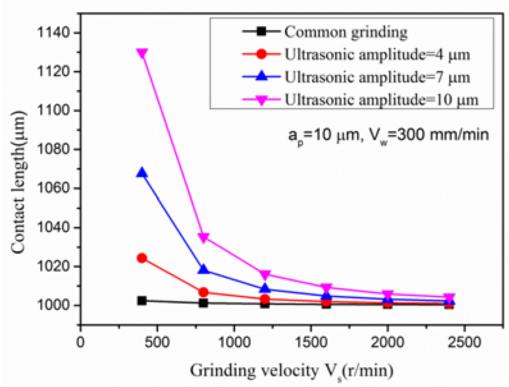

Fig. 9 Contact length versus grinding velocity for different ultrasonic amplitude

numerous small and straight grinding grooves, while the grinding grooves in UADG are sinusoidal shape and there is intermittent scratching owing to the ultrasonic vibration in the radial direction. Linear profiles of the ground surface along the grinding direction provide an insight into how the radial component of ultrasonic vibration qualitatively affects the surface topography.

Fig. 8 presents the linear profiles of the ground surface in DG and UADG at different ultrasonic vibration amplitudes. It can be found that the profile of DG is virtually flat while the profile fluctuates with periodic rise and fall in UADG. The greater the ultrasonic action is, the larger the value of peak-valley spacing will be, which could increase the surface roughness value. Therefore, the surface finish after UADG does not improve significantly and even becomes worse at a smaller value of grinding depth.

Beyond that, the axial component of ultrasonic vibration also exert a function on the surface roughness by changing the individual grinding traces as shown in Fig. 2(b). It can be found that the grits would interact with each other and more overlaps of the material removal could be generated due to the sinusoidal cutting trace, which can reduce the grinding marks and smooth the workpiece surface.[25,26] Moreover, due to the sinusoidal variations of the velocities in *y*- and *z*-direction, the impact effects of the tool on the workpiece are generated. The impact could produce tiny blade fragmentations of abrasive to get new cutting blades and thus the self-sharpening of the abrasives which is helpful for material removal during ultrasonic assisted grinding.[27,28] The ultrasonic vibration also increase the grain protrusion height and enlarges the chip allowance space by accelerating the removal rate of bond material.[29] The sharper grinding wheel is beneficial to improve the surface roughness. From that it can be inferred that the ultrasonic vibration in the axial direction tends to smoothen the surface topography and reduce the surface roughness. This can be considered as a main reason why the surface roughness is reduced in UADG at the grinding depth in the range of 10-20 μm.

As mentioned before, the ploughing action generated by ultrasonic vibration results in a worse surface topography, which means that the surface roughness should increase with the increase of the vibration amplitude and grinding depth. The integrated effects of ultrasonic vibration in the radial and axial direction result in the final workpiece surface. At the small depth of grinding, ultrasonic vibration has less effect on surface roughness improvement since the radial vibration is predominant. As the grinding depth increases, ultrasonic vibration can remarkably improve the surface roughness as the axial vibration generates more overlaps of the material removal than in DG. However, affected by the ploughing action owing to the axial vibration and deepening the grinding depth owing to the radial vibration, the surface roughness decreases first and then increases with the increase of ultrasonic vibration amplitude at the same grinding depth. When the grinding depth exceeds a certain value, the effect of ploughing caused by ultrasonic vibration surpasses the overlap effect, and then the surface roughness of UADG rises with the increase of grinding depth. The larger the ultrasonic amplitude is, the faster the growth rate becomes.

However, as shown in Fig. 9, with the increase of grinding velocity, the contact length of UADG and DG for a single grain would tend to equalize, which decreases the chance of the trajectories to cross each other. The effect of overlapping decreases. While the deepening effect is not weaker due to the grinding velocity has no effect on the radial vibration. Therefore, as the grinding velocity increases, the effect on surface roughness improvement gradually weakens and becomes even worse.

5. Conclusions

In this investigation, the ground surfaces are compared between DG and UADG with a large diameter grinding wheel. Due to the Poisson effect, the UADG using a large diameter grinding wheel is the combination of axial ultrasonic assisted grinding and radial ultrasonic assisted grinding. The radial vibration exerts a function on the increase of the surface roughness through deepening the individual grinding traces, and the axial vibration tends to smooth the surface topography by increasing the interaction overlap of adjacent cutting trajectories.

From the results of the experiments, the following conclusions can be obtained:

(1) In terms of surface quality, SEM micrographs reveal greater levels of overlapping and side flow/ploughing on the workpiece surface

machined with ultrasonic vibration in comparison with that of common grinding. Furthermore, the overlapping and side flow/ploughing were aggravated with the increase of vibration amplitude.

(2) The grinding depth and velocity have a great influence on ultrasonic effects. Slightly deep grinding depth and lower grinding velocity tend to produce a better surface at the same ultrasonic vibration frequency and amplitude.

(3) Under the current experimental conditions, the maxim reduction of surface roughness in UAG is 30% at the ultrasonic amplitude of 7 um and the grinding depth of 20 μm.

ACKNOWLEDGEMENT

The authors gratefully acknowledge the support of the National Natural Science Foundation of China (NSFC) through Grants No. 51605160, 51535012, U1604255, the support of the Key research and development project of Hunan province through Grants No. 2016JC 2001. The open Research Fund of Key Laboratory of High Performance Complex Manufacturing, Central South University (No.Kfkt2016-8).

REFERENCES

1. Sharma, A. K., Tiwari, A. K., and Dixit, A. R., "Effects of Minimum Quantity Lubrication (MQL) in Machining Processes Using Conventional and Nanofluid Based Cutting Fluids: A Comprehensive Review," Journal of Cleaner Production, Vol. 127, pp. 1-18, 2016.

2. Kumaran, S. T., Ko, T. J., Li, C., Yu, Z., and Uthayakumar, M., "Rotary Ultrasonic Machining of Woven CFRP Composite in a Cryogenic Environment," Journal of Alloys and Compounds, Vol. 698, pp. 984-993, 2017.

3. Shan, C., Zhang, X., Dang, J., and Yang, Y., "Rotary Ultrasonic Drilling of Needle-Punched Carbon/Carbon Composites: Comparisons with Conventional Twist Drilling and High-Speed Drilling," The International Journal of Advanced Manufacturing Technology, 2017. (DOI: 10.1007/s00170-017-1228-7)

4. Qi, H., Wen, D., Lu, C., and Li, G., "Numerical and Experimental Study on Ultrasonic Vibration-Assisted Micro-Channelling of Glasses Using an Abrasive Slurry Jet," International Journal of Mechanical Sciences, Vol. 110, pp. 94-107, 2016.

5. Qi, H., Wen, D., Yuan, Q., Zhang, L., and Chen, Z., "Numerical Investigation on Particle Impact Erosion in Ultrasonic-Assisted Abrasive Slurry Jet Micro-Machining of Glasses," Powder Technology, Vol. 314, pp. 627-634, 2017.

6. Watanabe, T., Sakuyama, H., and Yanagisawa, A., "Ultrasonic Welding between Mild Steel Sheet and Al-Mg Alloy Sheet," Journal of Materials Processing Technology, Vol. 209, Nos. 15-16, pp. 5475-5480, 2009.

7. Tawakoli, T. and Azarhoushang, B., "Influence of Ultrasonic Vibrations on Dry Grinding of Soft Steel," International Journal of Machine Tools and Manufacture, Vol. 48, No. 14, pp. 1585-1591, 2008.

8. Li, C., Zhang, F., Meng, B., Liu, L., and Rao, X., "Material Removal Mechanism and Grinding Force Modelling of Ultrasonic Vibration Assisted Grinding for SiC Ceramics," Ceramics International, Vol. 43, No. 3, pp. 2981-2993, 2017.

9. Gong, H., Fang, F., and Hu, X., "Kinematic View of Tool Life in Rotary Ultrasonic Side Milling of Hard and Brittle Materials," International Journal of Machine Tools and Manufacture, Vol. 50, No. 3, pp. 303-307, 2010.

10. Chen, H., Tang, J., Lang, X., Huang, Y., and He, Y., "Influences of Dressing Lead on Surface Roughness of Ultrasonic-Assisted Grinding," The International Journal of Advanced Manufacturing Technology, Vol. 71, Nos. 9-12, pp. 2011-2015, 2014.

11. Abdullah, A., Sotoodezadeh, M., Abedini, R., and Fartashvand, V., "Experimental Study on Ultrasonic Use in Dry Creep-Feed Up-Grinding of Aluminum 7075 and Steel X210Cr12," International Journal of Precision Engineering and Manufacturing, Vol. 14, No. 2, pp. 191-198, 2013.

12. Molaie, M., Akbari, J., and Movahhedy, M., "Ultrasonic Assisted Grinding Process with Minimum Quantity Lubrication Using Oil-Based Nanofluids," Journal of Cleaner Production, Vol. 129, pp. 212-222, 2016.

13. Paknejad, M., Abdullah, A., and Azarhoushang, B., "Effects of High Power Ultrasonic Vibration on Temperature Distribution of Workpiece in Dry Creep Feed up Grinding," Ultrasonics Sonochemistry, Vol. 39, pp. 392-402, 2017.

14. Chen, H., Tang, J., and Zhou, W., "An Experimental Study of the Effects of Ultrasonic Vibration on Grinding Surface Roughness of C45 Carbon Steel," The International Journal of Advanced Manufacturing Technology, Vol. 68, Nos. 9-12, pp. 2095-2098, 2013.

15. Chen, H. and Tang, J., "Influence of Ultrasonic Assisted Grinding on Abbott-Firestone Curve," The International Journal of Advanced Manufacturing Technology, Vol. 86, Nos. 9-12, pp. 2753-2757, 2016.

16. Wang, Y., Lin, B., Wang, S., and Cao, X., "Study on the System Matching of Ultrasonic Vibration Assisted Grinding for Hard and Brittle Materials Processing," International Journal of Machine Tools and Manufacture, Vol. 77, pp. 66-73, 2014.

17. Wei, S., Zhao, H., and Jing, J., "Investigation on Three-Dimensional Surface Roughness Evaluation of Engineering Ceramic for Rotary Ultrasonic Grinding Machining," Applied Surface Science, Vol. 357, pp. 139-146, 2015.

18. Cao, J., Wu, Y., Lu, D., Fujimoto, M., and Nomura, M., "Material Removal Behavior in Ultrasonic-Assisted Scratching of SiC Ceramics with a Single Diamond Tool," International Journal of Machine Tools and Manufacture, Vol. 79, pp. 49-61, 2014.

19. Li, S., Wu, Y., and Nomura, M., "Effect of Grinding Wheel Ultrasonic Vibration on Chip Formation in Surface Grinding of Inconel 718,"

The International Journal of Advanced Manufacturing Technology, Vol. 86, Nos. 1-4, pp. 1113-1125, 2016.

20. Chou, C.-L., “Wave Effects of Ultrasonic Vibration on Machining,” Pennsylvania State University, 1994.

21. Yanyan, Y., Bo, Z., and Junli, L., “Ultraprecision Surface Finishing of Nano-ZrO2 Ceramics Using Two-Dimensional Ultrasonic Assisted Grinding,” The International Journal of Advanced Manufacturing Technology, Vol. 43, Nos. 5-6, pp. 462-467, 2009.

22. Liang, Z., Wu, Y., Wang, X., and Zhao, W., “A New Two-Dimensional Ultrasonic Assisted Grinding (2D-UAG) Method and Its Fundamental Performance in Monocrystal Silicon Machining,” International Journal of Machine Tools and Manufacture, Vol. 50, No. 8, pp. 728-736, 2010.

23. Chen, J. B., Fang, Q. H., Wang, C. C., Du, J. K., and Liu, F., “Theoretical Study on Brittle-Ductile Transition Behavior in Elliptical Ultrasonic Assisted Grinding of Hard Brittle Materials,” Precision Engineering, Vol. 46, pp. 104-117, 2016.

24. Tang, J., Du, J., and Chen, Y., “Modeling and Experimental Study of Grinding Forces in Surface Grinding,” Journal of Materials Processing Technology, Vol. 209, No. 6, pp. 2847-2854, 2009.

25. Guo, B. and Zhao, Q., “Ultrasonic Vibration Assisted Grinding of Hard and Brittle Linear Micro-Structured Surfaces,” Precision Engineering, Vol. 48, pp. 98-106, 2017.

26. Wang, Y., Lin, B., Cao, X., and Wang, S., “An Experimental Investigation of System Matching in Ultrasonic Vibration Assisted Grinding for Titanium,” Journal of Materials Processing Technology, Vol. 214, No. 9, pp. 1871-1878, 2014.

27. Liang, Z., Wang, X., Wu, Y., Xie, L., Liu, Z., and Zhao, W., “An Investigation on Wear Mechanism of Resin-Bonded Diamond Wheel in Elliptical Ultrasonic Assisted Grinding (EUAG) of Monocrystal Sapphire,” Journal of Materials Processing Technology, Vol. 212, No. 4, pp. 868-876, 2012.

28. Wang, Q., Zhao, W., Liang, Z., Wang, X., Zhou, T., et al., “Investigation of Diamond Wheel Topography in Elliptical Ultrasonic Assisted Grinding (EUAG) of Monocrystal Sapphire Using Fractal Analysis Method,” Ultrasonics, Vol. 84, pp. 87-95, 2018.

29. Shen, J., Wang, J., Jiang, B., and Xu, X., “Study on Wear of Diamond Wheel in Ultrasonic Vibration-Assisted Grinding Ceramic,” Wear, Vols. 332-333, pp. 788-793, 2015.